Analyses of Temperature Behaviours at Fabrication Processes for Microaccelerometer Sensors

마이크로가속도계 센서의 제작공정에서 온도거동 해석

O. S. Kim

김 옥 삼

요 약 : 정전기력을 이용하는 마이크로가속도계 센서는 단결정 실리콘 SOI(Silicon On Insulator) 웨이퍼의 기판에 절전재료 적층과 등방성 및 이방성 부식공정으로 제작한다. 마이크로가속도 센서 개발에는 3차원 미소구조체의 제작공정에서 가열 및 냉각공정의 온도구배로 야기되는 포핑업과 같은 열변형 해석이 최적 형상설계에 중요한 요건이다. 본 연구에서는 양자역학적 현상인 턴널링전류 원리로 승용차 에어백의 검침부 역할을 하는 마이크로가속도 센서의 제조공정에서 소착현상을 방지하는 부가 비임과 턴널 갭의 FIB 절단가공과 백금 적층공정의 열적 거동을 해석한다. 마이크로머시닝 공정에서 온도의존성을 고려하여 연성해석하고 유한요소법의 상용코드인 MARC K6.1로 분석한 결과를 단결정 실리콘 웨이퍼로 가공하는 마이크로가속도 센서의 최적공정 및 형상설계를 위한 기초자료로 활용될 수 있을 것으로 기대된다.

1. Introduction

The remarkable progress in the technology of micromachining fabrication over the past 30 years has promoted the development of many type of silicon microsensor. These sensors have been utilized in wide applications such automotive, biomedical, aerospace and industrial engineering[1]. Micronization of sensor is a trend of the silicon sensor development with regard to a piezoresistive silicon pressure sensor, the size of the pressure sensor diaphragm has become smaller year by year, and a microaccelerometer with a size less than $200 \sim 300 \mu m$ has been realized. Recently, there has been growing interest in micromachined silicon accelerometers for applications to automotive equipment systems such as airbag, anti-lock brakingsystem(ABS), active suspension and navigation instru-

mentation[2]. Among them, airbag accelerometers open the most immediate and the largest market, whose demand for high reliability, mass production and high sensitivity to both velocity change and vibration cannot be met easily by conventional electromechanical sensor technology. For airbag applications, SCS (single crystal silicon) accelerometers show a strong potential due to simple detection circuit and moderate performance characteristics.

Over the past four or five years, numerical modeling of microsensors and microstructures have gradually been developed as a field of microelectromechanical system(MEMS) design process. The advantage of numerical analyses for prediction of device performance as well as device limitations has been verified in many problems[3]. In the design of microsensors and microstructures, a multitude of layers such as thermal oxide and coating are grown and deposited at different processes to achieve certain mechanical and/or electrical geomertris

and functions. Due to different mechanical and physical properties of these layers, the device usually experiences various thermal and mechanical loading resulting in displacements and residual stresses which are often not easy to predict by experimental approaches.

Successful analysis and design of the micro-accelerometer based on the tunnelling current concept using silicon on insulator (SOI) wafer depend on the knowledge about normal mechanical properties of the SCS layer such as yield stress, Young's modulus and Poisson's ratio, and their control through manufacturing process[4,5].

In this paper, we study some of the micro-machining processes of SCS for the micro-accelerometer, and their subsequent processeswhich might affect thermal and mechanical loads. The finite element method (FEM) has been a standard numerical modeling technique extensively utilized in structural engineering discipline for component design of micro-accelerometer. The FEM is becoming a standard design tool in microsensor industry[6,7].

## 2. Microaccelerometer based on tunnelling current concept

Silicon microfabricated accelerometers are being intensively developed because of the possibility of low cost batch fabrication. Fig. 1 shows a perspective of the microaccelerometer based on the tunnelling current concept, where a simple cantilever beam, paddle and supporting rims are micromachined from a SOI wafer (100) face. A Microaccelerometer based on tunnelling current concept has also been proposed, in which the sense signal is derived from a tunnelling current between a sensing tip and a counter electrode. Such accelerometers have a greater sensitivity than conventional capacitive accelerometers.

The paddle of microaccelerometer having a lot of holes due to etching has the following two roles, i. e. (1) carrying an extra proof mass to enhance inertia force, and (2) producing electro-static force as a part of condensor to control position as shown in Fig. 1 (b).
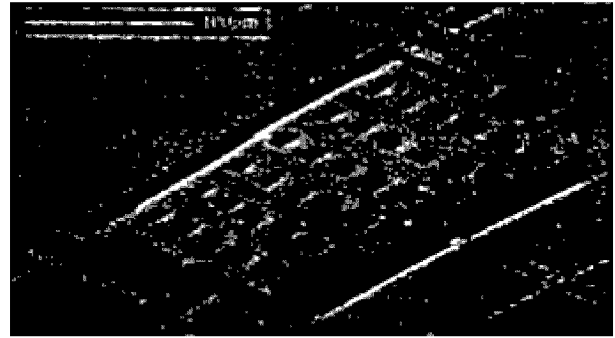
(a) SEM image for vibrating trial product of microaccelerometer.
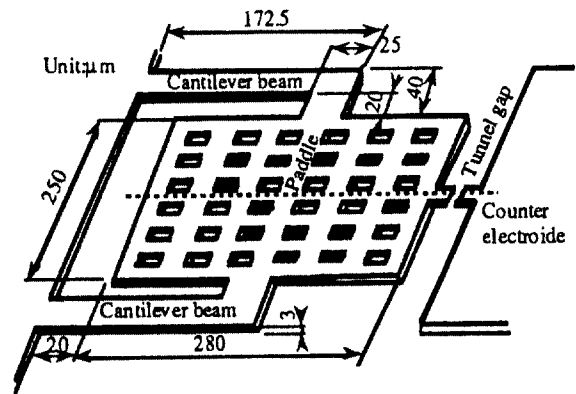
(b) Outline configuration

Fig. 1 Schematic view of microaccelerometer

The applied voltage must be less than 15 V, considering its supply resource. The change of applied acceleration is converted from the compensation voltage. Compensation voltage for the acceleration change should be about 0.3 V. The method of electrical activation, for maintaining a constant tunnel gap, consists of electrostatic pulling between the paddle and the silicon substrate.

3. Fabrication processes

In the fabrication of the microaccelerometer, SOI wafer is used as a starting material. SOI wafer is promising since the top layer silicon is SCS and no assembly after the processing is necessary. Only one lithographic step and simple wet etching are required to create microstruc-

ture[8].

3.1 SOI wafer production

The manufacturing process of SOI wafer consists of (1) growing a thermal oxide SiO_2 layer($2\mu m$) on a main substrate($500\mu m$) and a SiO_2 layer($2\mu m$) on a handle substrate(SCS) of paddle, (2) bonding a haddle substrate to a main substrate during 2hr[9] as shown in Fig. 3 (a).
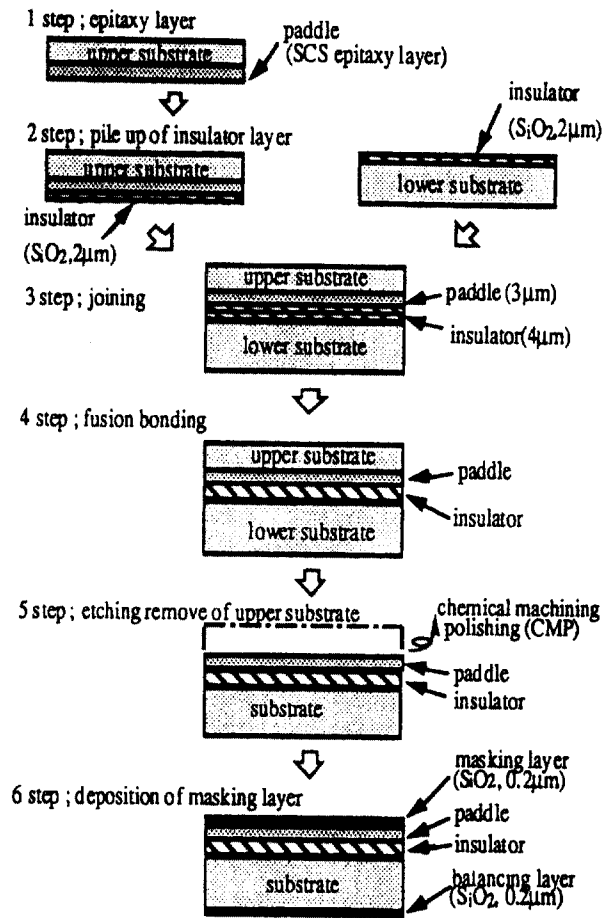
The bonding is achieved by attaching the oxidized surfaces of the two substrates eachother with pressure, and by inserting them into an oxidizing atmosphere at about $1000\sim1100°C$. Typically, the substrates are pressed together to expel most of air, bubble and void in between the bonded surfaces. The handle substrate is then thinned to some extent using micro grinding and chemical micro polishing(CMP) at room temperature. SOI wafer is promising since the top layer (thickness $3\mu m$) silicon is single crystalline and no assembly after the processing is necessary.
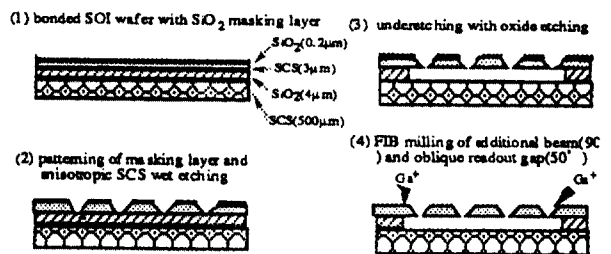
3.2 Fabrication steps

The fabrication steps for the microaccelerometer which are shown in Fig. 3 (b) can be summarized as follows : (1) oxidation of the SOI wafer to create a masking layer ($0.2\mu m$), (2) anisotropic wet etching of the top Si layer of 3 μm thickness with KOH, (3) wet etching in HF(conc.) to undercut the paddle($4\mu m$) with silicon oxide (SiO_2) layer, and (4) FIB(focused ion beam) cut to mill the tunnel gap and to fully release the paddle. The tunnel gap is machined to have a gap width of 200nm by the FIB technology. The deposition of an appropriate metal layer(Pt) will be necessary as a final step to assure good contact surface in the tunnel gap.

3.3 Popping up problem

Now the SOI wafer utilized has the proble that the paddle of microaccelerometer is popping up (max. $2\mu m$ at the sensing tip) after FIB cut as shown in Fig. 4. The reason for this popping up in paddle may be the thermal deformation according to some residual stress caused during the whole producing process mentioned above. The mechanical properties of SCS and SiO_2 are very important because the microaccelerometer is basically constructed on SOI wafer by the micro and nano technology of silicon[10].

(a) Schematic of SOI wafer producing process.

(b) Fabrication steps for the microaccelerometer

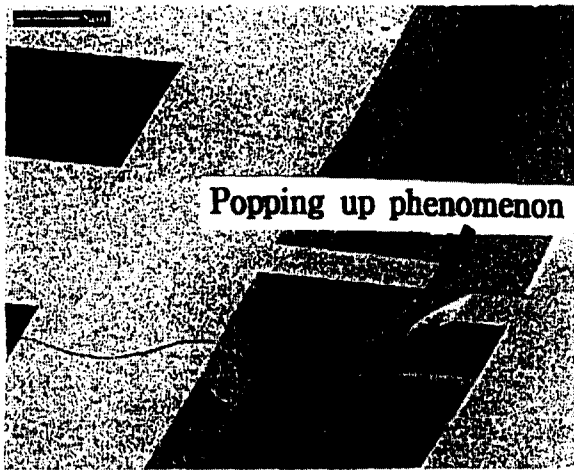Fig. 2 Schematic of SOI wafer producing process and fabrication steps

Fig. 3 Paddle popping up after FIB cut

4. Computational modeling

Algorithms of computational procedures for elasto-plastic residual stresses and deformations occurred in microaccelerometer manufacturing process are accurate for moderate strain in-crements as shown in Fig. 4. We seek for the general structure of the governing equation from cases 1 and 2. Let us assume the system under consideration can be separated into two inde- pendent temperature gradients and deformation subsystems.

Stress calculations also assume that the vertical temperature gradient in the micro-accelerometer can be ignored. In case 1, the thermal stress is caused due to the temperature gradient of SCS, SiO_2 and substrate with different thermal expansion coefficients. This is not discussed in this paper. In case 2, we consider the thermally epitaxial grown layer of oxide, the underetching of SiO_2 and the FIB milling of additional beam(90 °) and oblique tunnel gap (50°), refferring to Table 1.

The analytical approach to microsensors is only possible for simple structures. More com-plex shapes involing beams or multiple layer elements are best handled by finite element techniques. The paddle part is $280\mu m$ along, 250 μm wide and $3\mu m$ thick. In the analysis the
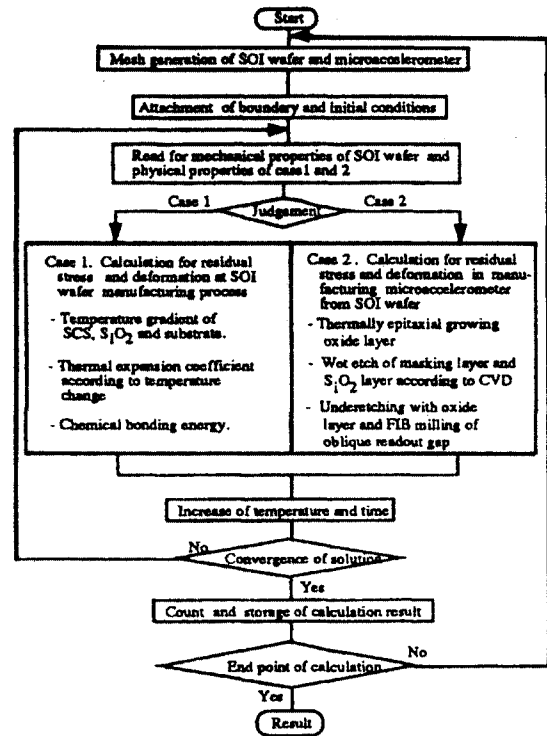

Fig. 4 Analysis flow for temperature gradients and deformations of SOI wafer and microaccelerometer

Table 1 Cyclic thermal loadings during micro-maching processes·

Process	Tempera-ture(℃)	Duration (sec)	Appliance	Working area	Note
Isotropic wet etching	25	About 1.3	HF	Masking layer	Not considered
Anisotropic wet etching	60	About 2.5	KOH	Silicon oxide layer	Not considered
FIB cutting	80	20	FIB	Additional beam	Considered
FIB cutting	100	54	FIB	Tunnel gap	Considered
Pt deposition	400	About 120	CVD	Tunnel gap	Considered

microaccelerometer volume is divided into 143 rectangular(8-node) elements. Analysis of this microaccelerometer using MARC K6.1 code, generates heat transfers and thermal stresses in a transient state[11].

5. Results and discussions

In Fig. 5, contours of z-direction displacement is plotted in the case of imitating the popping up phenomenon by applying a displacement controlled force at the tunnel gap. When the constraint is $2\mu m$ in the z-direction at the tunnel gap as shown in figure.

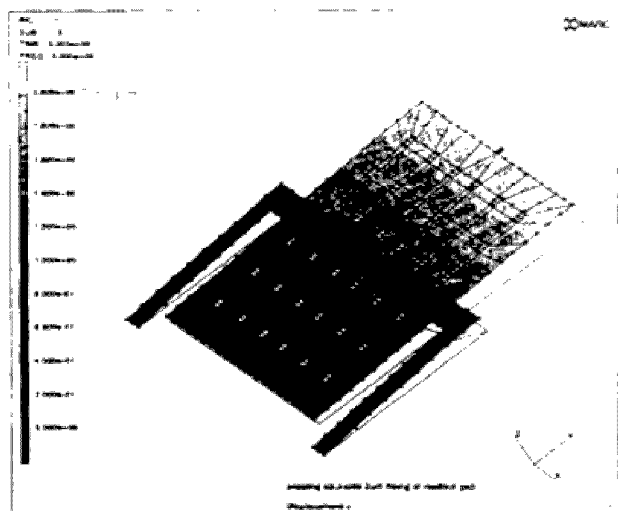at the bottom of paddle part.

Fig. 7 shows the calculated temperature profiles of microaccelerometer at the tunnel gap at heating after 2.2×10^{6} sec. The distributions illustrate the contours concentration of temperature near the corner of paddle according to heat source about $100°C$.
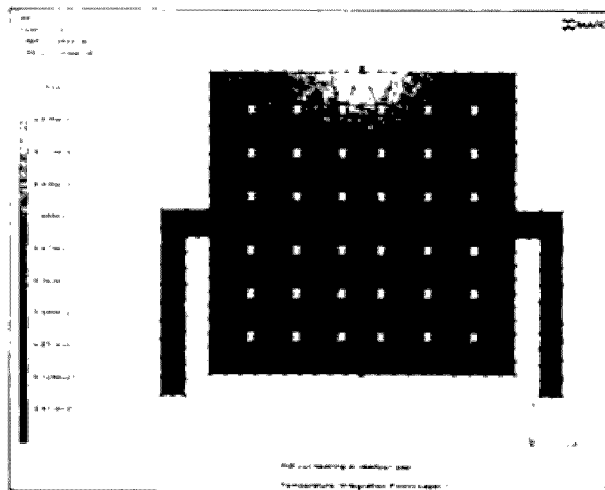

Fig. 5 Analysis of poping up at tunnel gap

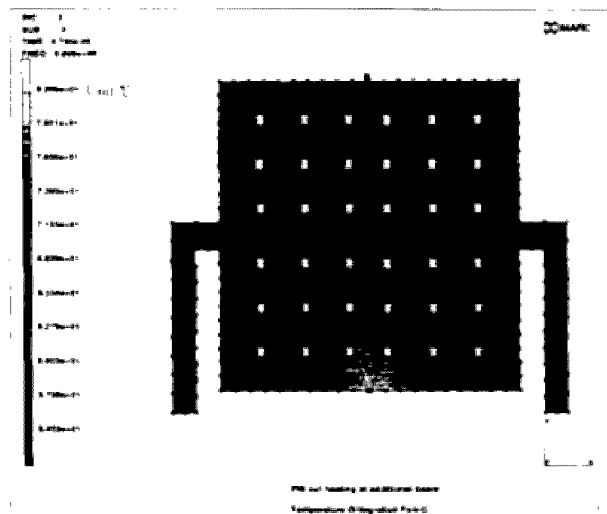Fig. 7 Temperature distribution after 2.24×10^{6} sec of heating process for tunnel gap by FIB cutting

Fig. 6 Temperature distribution after 4.7×10^{9} sec of heating process for additional beam by FIB cutting

Fig. 8 Temperature distribution after 4.7×10^{9} sec of heating process for tunnel gap by Pt drpositions

Fig. 6 shows the temperature distribution of a heating process for FIB cutting(90 °) at approximately heating after 4.8×10^{9} sec. Temperature rise sufficiently low at the suspended beams. Instead, larger temperature gradient can be seen
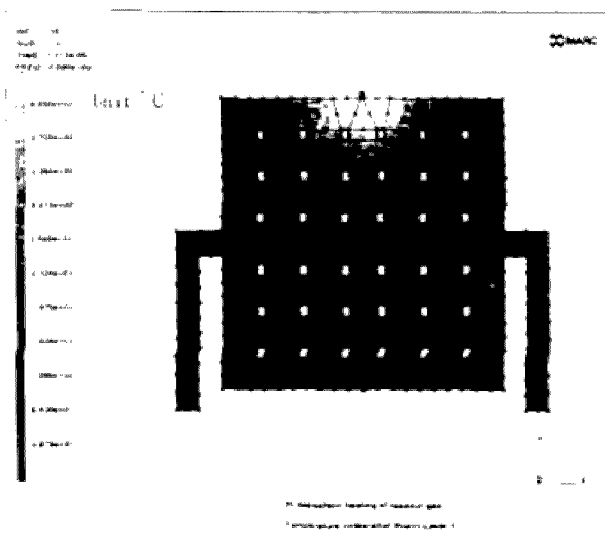
The temperature contours of Pt deposition heating process for the tunnel gap are depicted in Fig. 8 after 1.3×10^{6} sec. The typical heating behavior curves are shown in this figure.

Fig. 9 shows the temperature distributions of FIB cutting (90°) process at additional beam for preventing a sticking problem. The center of paddle part becomes about 5~20℃ higher than the corner of paddle and suspended beam edges.
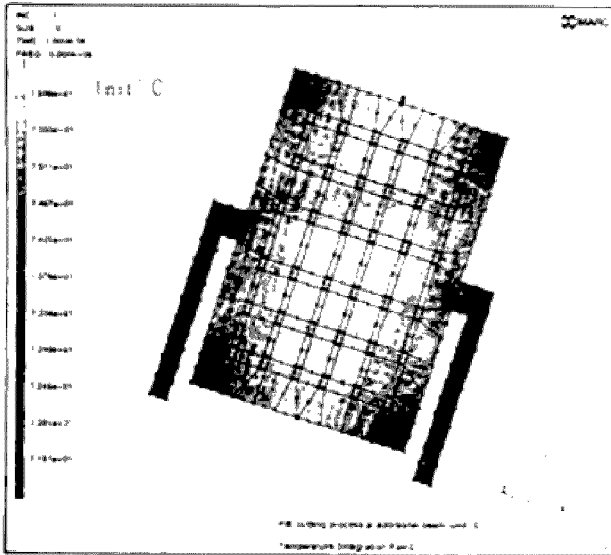

Fig. 9 Temperature distribution after 1.0×10^{6} sec of cooling process for additional beam by FIB cutting

Fig. 10 Temperature distribution after 1.133×10^{6} sec cooling process for tunnel gap by FIB cutting

Fig. 10 shows a calculated temperature distribution of microaccelerometer during a FIB cut cooling process after 1.1×10^{6} sec. Temperature gradients steep in the suspended beam edges

and the corner of paddle.

In Fig. 11, shows temperature contours representing the cooling process of Pt deposition. Corner parts of the paddle and the suspended beams are subjected to more thermal loss due to their corner shape. To obtain a more uniform temperature distribution, thermal radiation should be provided to these corner parts.
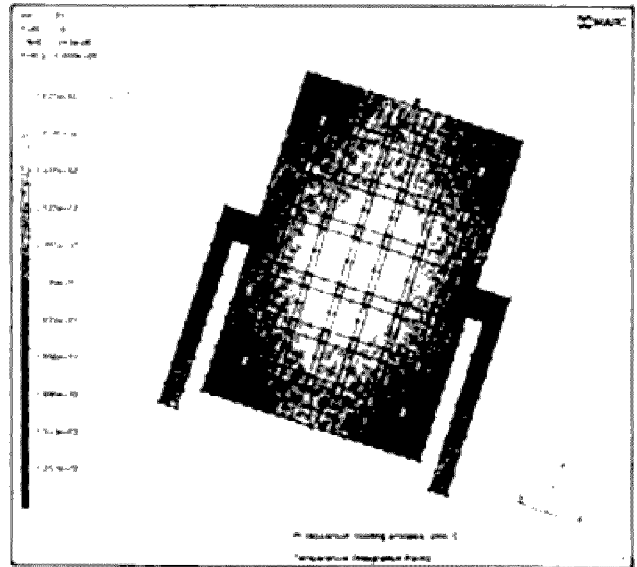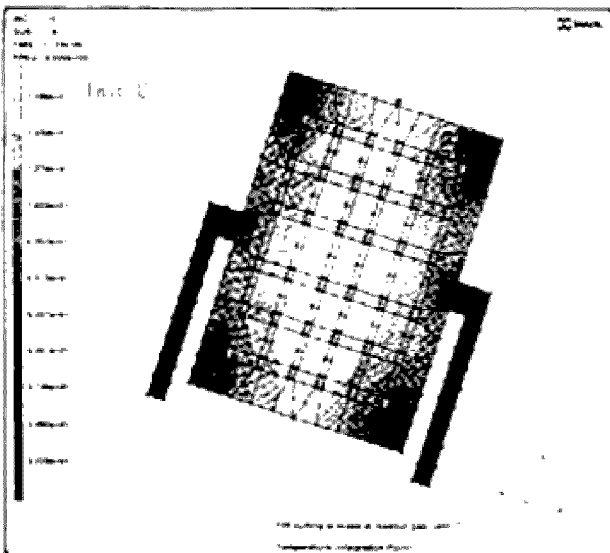

Fig. 11 Temperature distribution after 1.043×10^{6} sec of cooling process for tunnel gap by Pt deposition

6. Conclusions

One of major problems associated with the manufacturing processes of the microaccelerometer based on the tunnelling current concept is temperature gradient and thermal deformation. In this paper, we analyzed temperature and thermal behaviours occurred in the microaccelerometer during the FIB cutting process and the Pt deposition process.

Temperature rise sufficiently low at the suspended beams. Instead, larger temperature gradient can be seen at the bottom of paddle part. The center of paddle part becomes about 5~20℃ higher than the corner of paddle and suspended beam edges. Corner parts of the paddle and the suspended beams are subjected to more thermal loss due to their corner shape.

References

1. J. Bryzek, "Impact of MEMS Technology on Society", Sensors and Actuators, A 56, pp. 1~9, 1996

2. D. F. Moore, S. C. Burgess, H. Chiang, H. Klaubert, N. Shibaike and T. Kiriyama, "Micromachining and Focused Ion Beam Etching of Si for Accelerometer", Symposium on Micromachining and Microfabrication, SPIE, Vol. 2639, pp. 253~258, 1995

3. F. Pourahmadi, P. Barth and K. Peterse "Modeling of Thermal and Mechanical Stresses in Silicon Microstructures", Sensors and Actuators, A21-A23, pp. 850~858, 1990

4. J. Y. Richard, "Micro-machining using a Focused Ion Beam", Vacuum, Vol. 44 No.3/4, pp. 353~360, 1993

5. S. Johansson, F. Ericson and J. Schweitz, "Influence of Surface Coatings on Elasticity, Residual Stresses, and Fracture Properties of Silicon Microelements", J. Appl. Phys, Vol. 65, Jan. pp. 122~128, 1989

6. K. W. Lee and K. D. Wise, "SENSIM : A Simulation Program for Solid-State Pressure Sensors", IEEE. Transactions on Electron Devices, ED-29, pp. 34~41, 1982

7. S. Crary, O Juma and Y. Zhang, "Software Tools for Designers of Sensors and Actuator CAE Systems", IEEE. Solid-state sensors and Actuators (Transducers 91), San Francisco, CA, USA, p.498, 1991

8. Kurt E. Petersen, "Silicon as a Mechanical Materials", Proc. of IEEE, Vol. 70 No. 5, May, pp. 420~452, 1982

9. S. Johansson, J. Schweitz, L. Tenerz and J. Tiren, "Fracture Testing of Silico Microelements in situ in a Scanning Electron Microscope", J. Appl. Phys., Vol. 63(10), May, pp. 4799~4805, 1988

10. F. Ericson and J. Schweitz, "Micromechanical Fracture Strength of Silicon", J. Appl. Phys., Vol. 68(11), 1 Dec. pp. 5840~5846, 1990

11. MARC Analysis Research Corporation, MARC User's Manual K6.1 (1994).